ELSEVIER

Journal of Nuclear Materials 283–287 (2000) 768–772

journal of nuclear materials

www.elsevier.nl/locate/jnucmat

Comparative study of damage accumulation in iron under magnetic and inertial fusion conditions

E. Alonso [a,*], M.J. Caturla [a], T. Diaz de la Rubia [a], N. Soneda [b], J. Marian [c], J.M. Perlado [c], R.E. Stoller [d]

[a] *Lawrence Livermore National Laboratory, P.O. Box 808, L-369, Livermore, CA 94550, USA*
[b] *Central Research Institute of Electric Power Industry, Tokyo 201, Japan*
[c] *Instituto de Fusion Nuclear, Universidad Politecnica de Madrid, Madrid, Spain*
[d] *Oak Ridge National Laboratory, Oak Ridge, TN 37831-6376, USA*

Abstract

We present results of kinetic Monte Carlo (KMC) simulations of damage accumulation in Fe under conditions relevant to inertial (IFE) and magnetic fusion energy (MFE), with input obtained from molecular dynamics (MD). MD simulations provide information on the primary state of damage and were carried out for cascades with primary knock-on atom (PKA) energies ranging from 100 eV to 50 keV. These were used as input for a KMC simulation in which pulsed IFE irradiation and continuous MFE irradiation were simulated and compared. The MD collision cascades were introduced into the KMC simulation reproducing a recoil spectrum of 14 MeV neutrons. For pulsed irradiation, we discuss the manner in which damage accumulates depending on temperature and pulse rate. At low temperature, we show that there is no significant difference between pulsed and continuous irradiation when the integrated dose rate is the same.

1. Introduction

Reduced activation ferritic steels are one of the candidate materials for the first wall of future fusion devices. Therefore, understanding how damage is produced and accumulated is necessary to carefully assess their performance limits under irradiation. Transmission electron microscopy (TEM) studies have proven to be very successful in revealing the microstructural features produced by irradiation. Usually, pure metals are analyzed in order to deconvolute the effect of alloying elements. However, it seems to be a very difficult task in the case of pure iron irradiated with fusion neutrons. Unfortunately, the neutron sources currently available allow only low dose irradiation, where irradiation induced defects are still below the TEM resolution limit [1]. The situation is worse for inertial fusion energy (IFE). Its pulsed nature could have important consequences on damage accumulation but the only experimental evidence available on pulsed irradiation consists of swelling studies of ion irradiated samples [2]. Recently, Perkins [3] proposed a pulsed neutron source for irradiation experiments on small specimens under IFE-like conditions. Irradiation experiments could be performed as a function of variables such as temperature and pulse rate. This paper is intended to simulate irradiation conditions in such source and analyze the effect of pulse rate and temperature on damage accumulation, for a given pulse length and fixed dose rate during the pulse. The results will be qualitatively compared with past simulation work on the subject. Molecular dynamics (MD) simulations simulated the primary state of damage produced by fusion neutron irradiation. Defect migration kinetics were also obtained by MD simulations. In order to treat recoil spectrum and cascade features such as defect clustering in a full 3-D simulation, the MD results were supplied as input to a damage accumulation simulation by kinetic Monte Carlo (KMC). In addition, we used the same combination of

* Corresponding author. Tel.: +1-925 424 5850; fax: +1-925 422 2118.
E-mail address: edalonso@llnl.gov (E. Alonso).

0022-3115/00/$ - see front matter
PII: S0022-3115(00)00261-0

computational tools to simulate damage accumulation under magnetic fusion energy (MFE) conditions. In Section 2, we explain the methods used and, in Section 3, we show the IFE results and the comparative study with MFE.

2. Methods

Simulations of high energy displacement cascades, and of defect energetics and kinetics, were carried out with the MD simulation code, MDCASK [4]. The code runs in parallel under MPI on any number of platforms, including the 488 node IBM computer (ASCI Blue). The Langevin equation of motion [5] was applied to the atoms in the cell boundaries in order to control the temperature of the crystal.

The use of KMC to model defect diffusion during irradiation of materials has been rather sparse in the past, but the technique dates back over thirty years and was discussed extensively by Beeler [6]. The earliest reference to this method is the work of Besco in 1967 [7]. Doran [8] and Doran and Burnett [9] carried out short-term annealing simulations of displacement cascades in fcc and bcc Fe, respectively. More recently, Heinisch et al. [10–12] used a Monte Carlo code named ALSOME to model the migration, agglomeration and dissociation of the defects produced by 25 keV Cu self-irradiation at different temperatures. Within our own group, we have used our KMC code, BIGMAC, to model defect escape from cascades in Fe [13], V [14], Au [15] and Al [16].

Recently, we have described the BIGMAC code in detail [17,18]. In summary, BIGMAC is a computationally efficient KMC program that tracks the locations of defects, impurities, and clusters as a function of time. The starting point of these simulations is the primary damage state, i.e. the spatially correlated locations of vacancy and interstitials, obtained from MD simulations of displacement cascades. Each defect produced (including the clusters) has an activation energy for diffusion that can be extracted either from MD simulations or in some cases from experiments. The defects are allowed to execute random diffusion jumps (in one, two or three dimensions depending on the nature of the defect) with a probability proportional to their diffusivity. Similarly, dissociation rates from clusters are governed by a dissociation energy that includes the binding energy, E_b, of a particle to the cluster. The BIGMAC program requires input tables of D_0 and E_m for all mobile species, as well as the pre-factors and binding energies E_b for all possible clusters.

Input data on defect properties for Fe used here have been discussed in great detail in a recent publication [17] and will not be detailed here. Suffice it to say that single self-interstitial atoms (SIAs) and vacancies are mobile at all temperatures studied. In addition, SIA clusters are mobile in one dimension with an activation energy of 0.06 eV as determined by Soneda and Diaz de la Rubia [19], but get trapped by impurities with a binding energy of 1.1 eV that arises from elastic interaction. In our simulation, we assumed a concentration of impurities of 5 appm and we considered them immobile.

3. Discussion

The collision cascade database generated by two of the authors [13,20] was used for this study. The total number of defects produced in these cascades has been shown to be in very good agreement with experiment [21] and is approximately 1/3 of that predicted by the modified Kinchin–Pease model of Norgett, Robinson and Torrens (NRT) [22].

Each individual cascade results in a distribution of defects, some of which may be mobile depending on their properties and irradiation temperature. Because the KMC method takes into account all possible defect reactions at the correct rate depending on temperature, the simulations are ideal for evaluating the effects of pulsed irradiation on damage accumulation. After each pulse, the KMC computation allows the mobile defects to migrate and interact with other defects and traps for a time given by the pulse rate. Periodic boundary conditions are applied in all directions.

The simulated dose rate corresponds to 10^{15} n/cm^2/s integrated over time. The dose rate in the pulse itself is of the order of 1.4 dpa/s in Fe, and the pulse length is 1 μs. At 4 Hz, it results in a damage rate of 150 dpa/yr. The overall conditions are intended to simulate those that would be encountered if a material were irradiated with the laser-driven 14 MeV neutron source recently proposed by Perkins et al. [3]. The recoil spectrum used corresponds to the first wall of the MFE reactor Starfire [23] and was calculated with the SPECOMP/SPECTER code [24,25]. The probability function associated with each energy group and the energy groups of the spectrum were modified in two ways: (a) Electronic energy losses were subtracted from the primary knock-on atom (PKA) energy to include only damage energy. Robinson's approximation to Lindhard's theory was employed for this purpose [26]. (b) The energy groups of the recoil spectrum were changed to the PKA energies available in our MD database of recoils. The total energy deposited per neutron–iron collision was kept constant.

We should point out that the highest energy simulated by MD is 50 keV recoils of Fe in Fe, while the spectrum includes recoils of energies higher than 300 keV (after subtracting the electronic stopping). It is known that above approximately 20 keV cascades break up into subcascades of lower energy. The energy and spatial distribution of subcascades for recoils higher than 50 keV was estimated using TRIM [27].

Each microsecond pulse was simulated with six cascades picked at random with a probability of occurrence weighed by the modified recoil spectrum. For our KMC box of 300-nm edge length, this corresponds to instantaneous dose rates in the pulse of 1.4 dpa/s.

We simulated pulse repetition rates of 1, 10 and 100 Hz at 300 K. At this temperature, vacancies are mobile and small vacancy clusters dissociate. We also simulated pulsed irradiation at 100 Hz and 620 K, well within stage V, where vacancy clusters are unstable. For the MFE continuous irradiation, we chose a dose rate of 1.4×10^{-6} dpa/s, which is the expected in Starfire, and a temperature of 300 K to compare with the pulsed irradiation cases.

The main computational problem stems from the high mobility of SIA clusters that undergo 1-D glide. The cross-section for these clusters to participate in any reaction is rather low. Unfortunately, their low migration energy makes them a highly likely event that slows down the computation clock. In order to speed up the simulation, we opted for the following approximation. After the input of each cascade, a gliding direction is randomly determined for each of these 1-D migrating clusters. If they intersect any other defect in their trajectory, the reaction immediately occurs. If they do not, they are taken out of the simulation and put back in again when the next cascade arrives. Obviously, this approximation is valid only when few microstructural features are present, that is to say, at low dose.

Fig. 1 shows the concentration of vacancy clusters, Fig. 2 the concentration of interstitial clusters at trapping sites, Fig. 3 the concentration of sessile interstitial clusters, and Fig. 4 the average cluster size as a function of pulse rate and dose. In these plots, it is clearly seen that the longer the time between pulses, the lower the vacancy cluster concentration but the greater their size. The cluster density is not appreciably different between

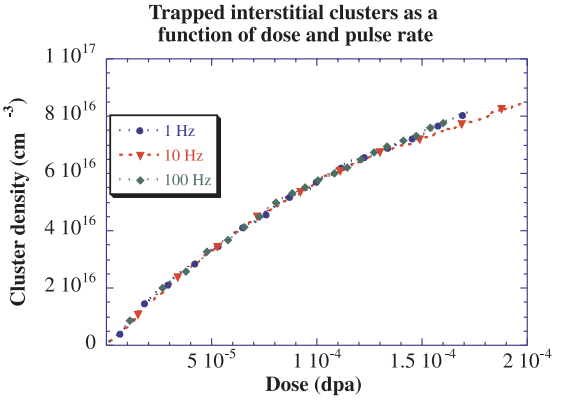

Fig. 2. Interstitial cluster density at traps as a function of dose for 1, 10, 100 Hz pulsed irradiation at 300 K.

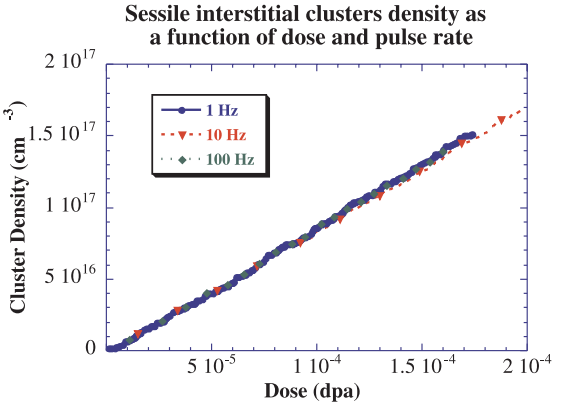

Fig. 3. Sessile interstitial clusters as a function of dose for 1, 10, 100 Hz pulsed irradiation at 300 K.

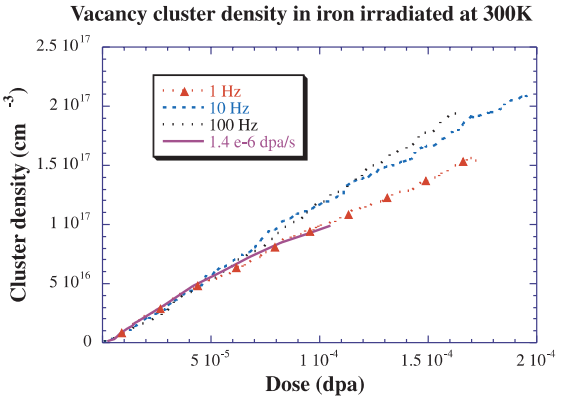

Fig. 1. Vacancy cluster density as a function of dose for 1, 10, 100 Hz pulsed irradiation and 1.4×10^{-6} dpa/s continuous irradiation at 300 K.

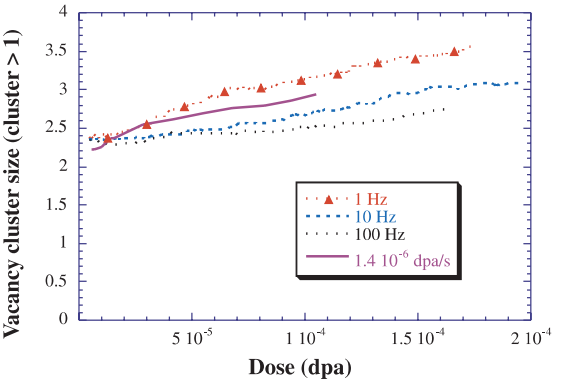

Fig. 4. Average vacancy cluster size as a function of dose for 1, 10, 100 Hz pulsed irradiation and 1.4×10^{-6} dpa/s continuous irradiation at 300 K.

the 1-Hz case and continuous irradiation, but the vacancy cluster size is larger for 1-Hz pulsed irradiation. Although their integrated doses are equal (1.4×10^{-6} dpa/s), the annealing time between pulses is 1 s at 1 Hz, whereas the time between cascades is only 0.16 s in the MFE case. The interstitial cluster density at traps is completely independent of the pulse rate and the same applies to the population of sessile interstitial clusters (sessile interstitial clusters are formed by the intersection of two gliding SIA clusters).

For pulsed irradiation, the sequence of events is as follows. The instantaneous dose rate during the pulse is so high that nothing occurs until the pulse is over. The annealing between pulses begins with the quick vacancy recombination with fast mobile interstitial clusters. This first stage spans over the first 0.5 s of the annealing and ends when all the SIA clusters have been trapped by impurities. That is why the concentration of interstitial clusters shows no pulse rate dependence, because their migration is so fast that all the events which involve interstitial clusters have already taken place before the arrival of the next pulse, independently of the pulse rate. At 300 K, the vast majority of trapped clusters are unable to overcome the detrapping barrier. From that moment until the next pulse, vacancies are free to move and cluster. Also, small vacancy clusters break up and drive cluster growth.

The temperature effect can be observed in Figs. 5 and 6 for pulsed irradiation at 100 Hz. At 620 K (Stage V), the vacancy cluster density is lower than at 300 K but their size larger. This is a consequence of the quick coarsening process with increasing temperatures. At 620 K the minimum vacancy cluster size allowed by temperature is considerably high. Thus, since cluster growth is faster at high temperatures, differences between pulsed and continuous irradiation are expected to be more pronounced.

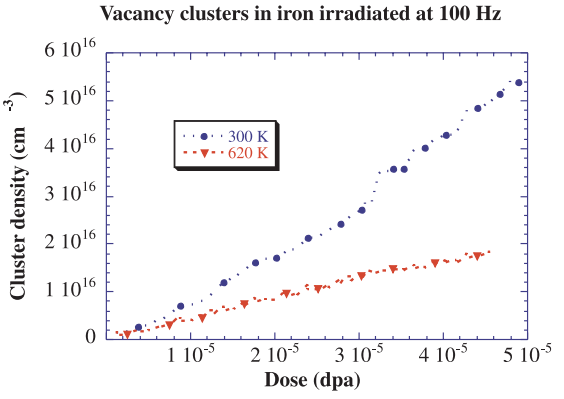

Fig. 5. Vacancy cluster density as a function of dose for 100 Hz pulsed irradiation at 300 and 620 K.

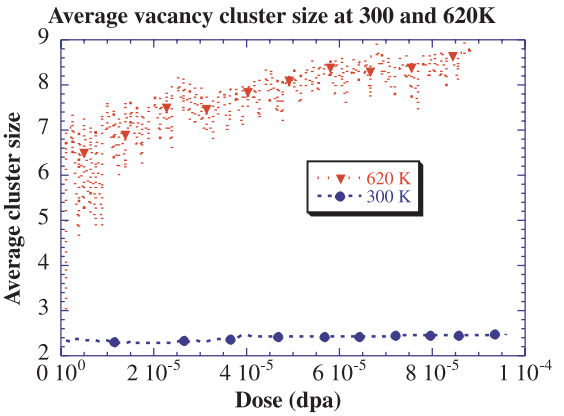

Fig. 6. Average vacancy cluster size as a function of dose for 100 Hz pulsed irradiation at 300 and 620 K.

Unfortunately, our results are not directly comparable with any experiments performed in the past. Most of the experimental work on pulsed irradiation in the literature concludes that pulsed irradiation reduces the void nucleation rate and alters the void growth rate [28]. No helium was included as an impurity in our study, so void nucleation and growth could not be studied. However, there is a considerable amount of work on pulsed irradiation based on kinetic rate theory. In his comparison of different pulsed irradiation systems, Ghoniem (1980) concluded that the concentration of loops was higher in pulsed systems than in continuously irradiated environments [29]. This is in clear disagreement with our results. Nevertheless, the fast interstitial cluster migration, responsible for the independence of cluster density and pulse rate, was not contemplated in Ghoniem's study.

4. Conclusions

We have presented a study of pulsed irradiation in Fe under conditions relevant to IFE and MFE. We analyzed the influence of pulse rate and temperature in the context of defect production and clustering. At 300 K, we observe that there is almost no difference between pulsed and continuous irradiation for the same integrated dose rate. Also, as it was expected, time between pulses is the variable that controls vacancy cluster density and size. Vacancy cluster densities are lower for low pulse rates but their sizes are larger. In addition, we show the influence of temperature on these processes. Not surprisingly, vacancy cluster growth is assisted by high temperatures. We also find the behavior of interstitial clustering independent of pulse rate, which is in disagreement with other simulations existing in the literature. We ascribe this difference to the fast interstitial cluster migration, which was not included in past studies.

Acknowledgements

We have benefited from discussions with L. John Perkins. This work was carried out under the auspices of the US Department of Energy by Lawrence Livermore National Laboratory under contract W-7405-Eng-48 and was supported by the Office of Fusion Energy Sciences.

References

[1] T. Yoshiie, Y. Satoh, H. Taoka, S. Kojima, M. Kiritani, J. Nucl. Mater. 155–157 (1988) 1098.
[2] N.H. Packan, Radiat. Eff. 101 (1986) 189.
[3] L.J. Perkins et al., Fus. Technol., to be published.
[4] M.J. Caturla, B. Chan, D. Nielsen, T. Diaz de la Rubia, unpublished.
[5] R. Biswas, D.R. Hamann, Phys. Rev. B 34 (1986) 895.
[6] J.R. Beeler Jr., Radiat. Eff. Comput. Exp., North-Holland, Amsterdam, 1983.
[7] D.G. Besco, Computer Simulation of Point Defect Annealing in Metals, USA-AEC Report GEMP-644, October 1967.
[8] D.G. Doran, Radiat. Eff. 2 (1970) 249.
[9] D.G. Doran, R.A. Burnett, in: P.C. Gehlen, J.K.R. Beeler Jr., R.I. Jafee (Eds.), Interatomic Potentials and Simulation of Lattice Defects, Plenum, New York, 1972, p. 403.
[10] H.L. Heinisch, B.N. Singh, T. Diaz de la Rubia, J. Nucl. Mater. 127 (1994) 212.
[11] H.L. Heinisch, Nucl. Instrum. and Meth. B 102 (1995) 47.
[12] H.L. Heinisch, B.N. Singh, J. Nucl. Mater. 251 (1997) 77.
[13] N. Soneda, T. Diaz de la Rubia, Philos. Mag. A 78 (1998) 995.
[14] E. Alonso, M.-J. Caturla, T. Diaz de la Rubia, J.M. Perlado, J. Nucl. Mater. 276 (2000) 221.
[15] T. Diaz de la Rubia, N. Soneda, M.-J. Caturla, E. Alonso, J. Nucl. Mater. 251 (1997) 13.
[16] A. Almazouzi, M.-J. Caturla, M. Alurralde, T. Diaz de la Rubia, M. Victoria, Nucl. Instrum. and Meth. B 153 (1999) 105.
[17] M.-J. Caturla, N. Soneda, E. Alonso, B. Wirth, T. Diaz de la Rubia, J.M. Perlado, J. Nucl. Mater. 276 (2000) 13.
[18] M.D. Johnson, M.J. Caturla, T. Diaz de la Rubia, J. Appl. Phys. 94 (1998) 1963.
[19] N. Soneda, T. Diaz de la Rubia, Philos. Mag. A, submitted.
[20] R.E. Stoller, A.F. Calder, presented at 9th Int. Conf. on Fusion Reactor Materials, Colorado Springs, CO, USA, Oct. 1999.
[21] R.S. Averback, T. Diaz de la Rubia, in: F. Spaepen, H. Ehrenreich (Eds.), Solid State Physics, vol. 51, Plenum, New York, 1998.
[22] M.J. Norgett, M.T. Robinson, I.M. Torrens, Nucl. Eng. Des. 33 (1975) 50.
[23] Argonne National Laboratory, McDonnell Douglas Astronautics, General Atomic, and the Ralph M. Parsons, STARFIRE: A Commercial Tokamak Fusion Power Study, Argonne National Lab, Argonne, IL, ANL/FPP-80-1, 1980.
[24] L.R. Greenwood, SPECOMP Calculations of radiation damage in compounds, ASTM-STP 1001 (1989) 598–602.
[25] L.R. Greenwood, R.K. Smither, SPECTER: neutron damage calculations for materials irradiations, ANL/FPP-TM-197, 1985.
[26] M.T. Robinson, J. Nucl. Mater. 216 (1994) 1.
[27] J.P. Biersack, L. Haggmark, Nucl. Instrum. and Meth. 194 (1982) 93.
[28] N.M. Ghoniem, G.L. Kulcinsky, Nucl. Technol./Fus. 2 (1982) 165.
[29] N.M. Ghoniem, J. Nucl. Mater. 89 (1980) 359.